Spin Dynamics in Pyrochlore Heisenberg Antiferromagnets

P. H. Conlon* and J. T. Chalker

Theoretical Physics, Oxford University, 1 Keble Road, Oxford, OX1 3NP, United Kingdom

(Received 9 April 2009; published 12 June 2009)

We study the low temperature dynamics of the classical Heisenberg antiferromagnet with nearest neighbor interaction on the frustrated pyrochlore lattice. We present extensive results for the wave vector and frequency dependence of the dynamical structure factor, obtained from simulations of the precessional dynamics. We also construct a solvable stochastic model for dynamics with conserved magnetization, which accurately reproduces most features of the precessional results. Spin correlations relax at a rate independent of the wave vector and proportional to the temperature.

DOI: 10.1103/PhysRevLett.102.237206 PACS numbers: 75.40.Gb, 75.10.Hk, 75.40.Mg

Geometrical frustration in magnets inhibits ordering. Simple, classical models for these systems have very degenerate ground states [1,2]. Reflecting this degeneracy, highly frustrated magnetic materials characteristically remain in the paramagnetic phase even at temperatures low compared to the scale set by exchange interactions. The behavior in this cooperative paramagnetic regime has been the focus of much recent research [3,4].

Nearest neighbor antiferromagnets on the pyrochlore lattice with classical n-component spins are representative of a large class of models [5,6]. They have remarkable correlations at low temperature, which are intermediate between those of conventionally ordered and completely disordered systems. These can be understood by mapping spin states onto configurations of a vector field, or *flux field*, which is solenoidal for ground states [7–9]. Gaussian fluctuations of this flux field provide a coarse-grained description of the cooperative paramagnet. Static spin correlations have a power-law dependence on separation, inside a correlation length ξ that diverges as temperature T approaches zero. These correlations result in sharp features, termed *pinch points*, in diffuse scattering as a function of wave vector.

The dynamics of cooperative paramagnets has not been studied as extensively as the statics, but some ingredients are clear. In a Heisenberg model with precessional dynamics, the short-time behavior can be viewed in terms of harmonic spin wave fluctuations in the vicinity of a specific ground state, while over longer times the system wanders around the ground-state manifold. This second component to the motion results in decay of the spin autocorrelation function at long times, with a decay rate shown to be linear in T using simulations and phenomenological arguments [5]. These theoretical ideas are supported by inelastic neutron scattering measurements on pyrochlore antiferromagnets: an early study of $CsNiCrF_6$ revealed strong temperature dependence to the width in energy of quasielastic scattering for $T < |\Theta_{CW}|$ [10], while recent work on $Y_2Ru_2O_7$ shows a width linear in T as predicted [11].

Our aim in this Letter is to establish a much more comprehensive description of cooperative paramagnets with precessional dynamics than has been available so far. The topic is interesting from several perspectives. First, in view of the pinch points in static correlations, it is natural to ask about the wave vector dependence of the dynamical structure factor, accessible in single-crystal measurements. Little is currently known about this: the autocorrelation function of Ref. [5] is expressed as an integral over all wave vectors, while the measurements of Ref. [11] used a powder sample. Second, dynamics in the paramagnetic phase of unfrustrated antiferromagnets is dominated by spin diffusion [12–14], and one would like to know whether this extends to the cooperative paramagnet. Third, behavior in the Heisenberg model should be compared to that in spin ice, which is represented by the Ising pyrochlore antiferromagnet with dynamics controlled by the motion of monopole excitations [15].

In outline, our results are as follows. We find at low temperature three types of behavior in different regions of reciprocal space. (i) Close to reciprocal lattice points, correlations are dominated by spin diffusion with a temperature-independent diffusion constant. (ii) At a generic wave vector [not included in (i) or (iii)] correlations are Lorentzian in frequency with a width linear in T and independent of wave vector. (iii) Close to nodal lines in reciprocal space on which the static, ground-state structure factor vanishes [8], dynamical correlations are dominated by finite-frequency spin wave contributions. This picture is hence very different from that for the kagome Heisenberg antiferromagnet, which shows order-by-disorder and propagating modes [16].

We consider the classical Heisenberg antiferromagnet with nearest neighbor interactions on the pyrochlore lattice. Lattice sites (labeled i, j) form corner-sharing tetrahedra (labeled α, β). Spins $\mathbf{S}_i$ are unit vectors and $\mathbf{L}_\alpha = \sum_{i\in\alpha}\mathbf{S}_i$ is the total spin of tetrahedron α. The Hamiltonian is

$$H = J\sum_{\langle ij\rangle}\mathbf{S}_i\cdot\mathbf{S}_j \equiv \frac{1}{2}J\sum_{\alpha}\mathbf{L}_\alpha^2 + c, \qquad (1)$$

where c is a constant. Ground states satisfy $\mathbf{L}_\alpha = 0$ for all

α. The equation of motion, describing precession of each spin around its local exchange field, is

$$\frac{d\mathbf{S}_i}{dt} = -J\mathbf{S}_i \times \sum_j \mathbf{S}_j, \tag{2}$$

where sites j are the nearest neighbors of i. The global spin rotation symmetry of Eq. (1) implies conservation of total spin in the dynamics.

Before presenting results from a molecular dynamics study of Eq. (2), we consider an analytically tractable stochastic model for the dynamic behavior. It is known that static spin correlators for the classical Heisenberg model are well described by those for n-component spins in the large n limit [6,7]. Building on this, we set out to endow the $n = \infty$ model with appropriate dynamics. First we recall some details of the static model. Taking the second form of the Hamiltonian in Eq. (1), a single spin component in the large n limit has the unnormalized probability distribution $e^{-\beta E}$ with

$$\beta E = \frac{1}{2}\sum_i \lambda s_i^2 + \frac{1}{2}\beta J \sum_\alpha l_\alpha^2, \tag{3}$$

where now $l_\alpha = \sum_{i\in\alpha} s_i$ is the sum of "soft" spins ($-\infty < s_i < \infty$) on tetrahedron α. The spin length is constrained by the Lagrange multiplier λ. For $\beta \to \infty$, the second term in Eq. (3) enforces all the l_α to be zero. The interaction term written directly in terms of the spins is $\frac{1}{2}\beta J \sum_{ij}(A_{ij} + 2\delta_{ij})s_i s_j$, where A_{ij} is the adjacency matrix for the pyrochlore lattice. We call the combination $A_{ij} + 2\delta_{ij}$ the interaction matrix. Its eigenvalues $\upsilon_\mu(\mathbf{q})$ are labeled by wave vector $\mathbf{q}$ and a band index $\mu \in \{1, 2, 3, 4\}$. Two bands are flat [$\upsilon_{1,2}(\mathbf{q}) = 0$] and two ($\mu = 3, 4$) are dispersive. Requiring $\langle s_i^2\rangle = 1/3$ to mimic behavior of a single spin component in the Heisenberg model, $\lambda = 3/2 + \mathcal{O}(T/J)$ for $T \ll J$. We denote the Fourier transform of the spin variables s_i by $s_\mathbf{q}^a$, where a is a sublattice index, and define the sublattice sum $s_\mathbf{q} = \sum_{a=1}^4 s_\mathbf{q}^a$. Transforming from $s_\mathbf{q}^a$ to the basis (denoted by tildes) that diagonalizes the interaction matrix gives collective spin variables $\tilde{s}_\mathbf{q}^\mu$. We want to introduce time dependence and calculate the dynamic correlation function $S(\mathbf{q}, t) = \langle s_\mathbf{q}(t) s_\mathbf{q}^*(0)\rangle$, and its time Fourier transform, the dynamic structure factor $S(\mathbf{q}, \omega)$, measured using neutron scattering.

There are many choices of dynamics which reproduce any given equilibrium distribution. To approximate Eq. (2) we demand a local dynamics that conserves the total spin. We can ensure this by requiring the spin on each site to satisfy a local continuity equation. We introduce spin currents on bonds of the pyrochlore lattice, which have drift and noise terms. We take the drift current on a bond linking two sites to be proportional to the difference in the generalized forces $\partial E/\partial s_i$ at the sites. This favors relaxation towards a configuration that minimizes E; the thermal ensemble is maintained by noise which has an independent Gaussian distribution on each bond. These assumptions lead to the dynamical equations for the soft spins

$$\frac{ds_i}{dt} = \Gamma \sum_l \Delta_{il}\frac{\partial E}{\partial s_l} + \zeta_i(t), \tag{4}$$

where the matrix Δ is the lattice Laplacian (for a lattice with coordination number z, $\Delta_{il} = A_{il} - z\delta_{il}$). The correlator of the noise $\zeta_i(t)$ at site i, $\langle \zeta_i(t)\zeta_j(t')\rangle = 2T\Gamma\Delta_{ij}\delta(t - t')$, has an amplitude fixed by the requirement of thermal equilibrium. The only free parameter in the model is the rate Γ, which sets a time scale for dynamical processes. The Langevin equation (4) is straightforward to solve in the diagonal basis. It gives the correlation function

$$\langle \tilde{s}_\mathbf{q}^\mu(t)\tilde{s}_{-\mathbf{q}}^\nu(0)\rangle = \frac{\delta_{\mu\nu}T}{J\upsilon_\mu + \lambda T} e^{-\Gamma(8-\upsilon_\mu)(J\upsilon_\mu+\lambda T)t}. \tag{5}$$

The dynamic correlation function is then

$$S(\mathbf{q}, t) = \sum_{\mu=1}^4 g_\mu(\mathbf{q})\langle \tilde{s}_\mathbf{q}^\mu(t)\tilde{s}_{-\mathbf{q}}^\mu(0)\rangle, \tag{6}$$

where the structure factors $g_\mu(\mathbf{q})$ are formed from the eigenvectors of the interaction matrix. They satisfy the sum rule $\sum_{\mu=1}^4 g_\mu(\mathbf{q}) = 4$.

For completeness we present their explicit forms here. In the notation of [7], where $c_{ab} = \cos(\frac{q_a+q_b}{4})$ and $c_{\overline{ab}} = \cos(\frac{q_a-q_b}{4})$ with $Q = c_{xy}^2 + c_{\overline{xy}}^2 + c_{yz}^2 + c_{\overline{yz}}^2 + c_{xz}^2 + c_{\overline{xz}}^2 - 3$ and defining $P \equiv \sqrt{1+Q}$, the eigenvalues of the interaction matrix are $\upsilon_{1,2} = 0$ and $\upsilon_{3,4} = 4 \mp 2P$. Further defining $s_a^2 \equiv \sin^2(\frac{q_a}{4})$ and $c_{(ab)} \equiv c_{ab} + c_{\overline{ab}}$, the $g_\mu(\mathbf{q})$ are for the degenerate flat bands

$$g \equiv g_1 + g_2 = 2 - \frac{4}{3-Q}\left[c_{(xy)}s_z^2 + c_{(yz)}s_x^2 + c_{(zx)}s_y^2\right]$$

and for the dispersive bands

$$g_{3,4} = 2 - \frac{1}{2}g(1 \pm 2P^{-1}) \pm P^{-1}(2 - c_{(yz)} - c_{(xz)} - c_{(xy)})$$

which indeed satisfy $g_1 + g_2 + g_3 + g_4 = 4$.

We now examine the implications of this model for $T \ll J$, emphasizing the features (i)–(iii) mentioned in our introduction. From the exponent in Eq. (5) we obtain a characteristic time for decay of correlations. (i) In the vicinity of $\mathbf{q} = 0$ only the coefficient $g_4(\mathbf{q})$ is nonzero and so behavior is controlled by the fourth band whose decay rate is $\tau^{-1} = 8\Gamma J a^2 q^2 + \mathcal{O}(q^4)$, where a is the pyrochlore site spacing; from this we identify the spin diffusion constant in this model as $D = 8\Gamma J a^2$, independent of T. (ii) At a generic wave vector where g_1 and g_2 are nonzero, most of the spectral weight is in the flat bands, with decay rate $\tau^{-1} = 8\Gamma\lambda T$, independent of q; in an approximation where only the flat bands contribute, this implies the dynamic structure factor factorizes as $S(\mathbf{q}, \omega) = S(\mathbf{q})f(\omega)$, a possibility noted in [6]. (iii) On

nodal lines [8], high symmetry directions in reciprocal space along which $g_1(\mathbf{q}) + g_2(\mathbf{q}) = 0$, the decay rate is wave vector dependent and $\mathcal{O}(J)$ away from $\mathbf{q} = 0$.

To test these ideas we have performed simulations of the full precessional dynamics, Eq. (2). Low T configurations are obtained using a Metropolis Monte Carlo sampling method. We take these as initial configurations for numerical integration of the equations of motion using a fourth-order Runge-Kutta algorithm with adaptive step size. Energy and total spin are conserved to relative errors no greater than 10^{-6}. We report data from simulations on system sizes with total number of sites $N = 4L^3$ for $L = 16, 32$. We calculate the dynamic correlation function $S(\mathbf{q}, t) \equiv \langle \mathbf{S}_{\mathbf{q}}(t) \cdot \mathbf{S}_{-\mathbf{q}}(0) \rangle$ and the dynamical structure factor $S(\mathbf{q}, \omega) \equiv \langle |\mathbf{S}_{\mathbf{q}}(\omega)|^2 \rangle$, where $\mathbf{S}_{\mathbf{q}} = \sum_{a=1}^{4} \mathbf{S}_{\mathbf{q}}^a$ is the Fourier transformed spin configuration and a runs over the four sublattices. We present results under the headings (i)–(iii) as above, expressing $\mathbf{q}$ in reciprocal lattice units as $\mathbf{q} = 2\pi\mathbf{k}$ for Figs. 2–4.

(i) Since the total magnetization is conserved, one expects diffusion at sufficiently small q. The simulations confirm diffusive behavior with a diffusion constant independent of temperature. At small q, the data should collapse onto the scaling form appropriate for diffusion,

$$\beta q^2 S(\mathbf{q}, \omega) = 3\chi \frac{2D}{(\omega/q^2)^2 + D^2}, \tag{7}$$

where χ is the susceptibility per primitive unit cell and the factor of 3 is due to the three spin components. Figure 1 shows this scaling collapse when plotted as in Eq. (7), and demonstrates that the diffusion constant is independent of temperature. The prediction of Eq. (6), whose small q limit has precisely the form of Eq. (7), is an excellent fit with $\Gamma = 0.167$.

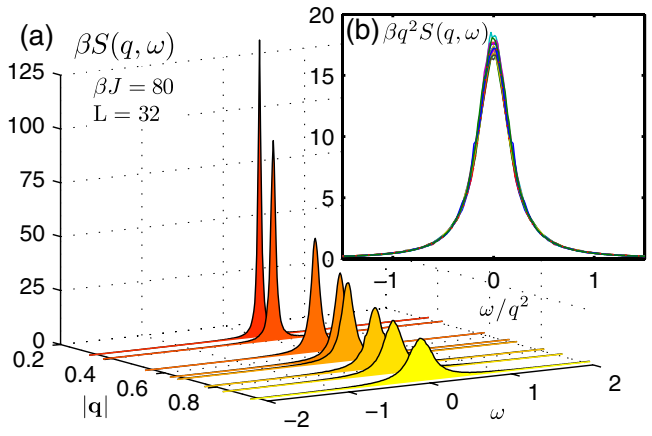

FIG. 1 (color online). Evidence for spin diffusion. (a) Dependence of $S(q, \omega)$ on q and ω at small q. (b) Scaling collapse following Eq. (7) at multiple temperatures ($\beta J = 20, 40, 60, 80$) and four of the wave vectors plotted in (a). Also plotted is the prediction of Eq. (6).

(ii) At a generic point in reciprocal space (not near $\mathbf{q} = 0$ or a nodal line) the structure factor is well described by a Lorentzian centered on $\omega = 0$, indicating relaxational dynamics (Fig. 2, upper inset). The decay rate for this relaxation (Fig. 2, main panel) is proportional to T and independent of the wave vector, even close to the pinch points.

(iii) On nodal lines, by contrast, the width in frequency of $S(\mathbf{q}, \omega)$ is $\mathcal{O}(J)$ and depends little on T; see Fig. 2, lower inset. High frequency ($\omega = 2.5J$) and zero frequency behavior is also presented in Fig. 3, as a survey of $S(\mathbf{q}, \omega)$ in the (q_x, q_x, q_z) plane, using data taken at $\beta J = 500$ and typical of all low temperatures. Weight in $S(\mathbf{q}, \omega)$ at $\omega \sim J$ and low T can be viewed as due to spin wave fluctuations in the vicinity of an instantaneous ground state. In contrast to behavior in the kagome antiferromagnet [16], there is no evidence in Fig. 3 for sharp propagating modes.

We next demonstrate that the stochastic model accurately reproduces most aspects of the precessional dynamics. We examine behavior with each type of dynamics at different temperatures and times along a path in the Brillouin zone: $\mathcal{P} = (0, 0, 0) \xrightarrow{\mathcal{P}_1} (2, 2, 2) \xrightarrow{\mathcal{P}_2} (0, 0, 2)$. This consists of the section $\mathcal{P}_1$ along high symmetry nodal lines passing through a pinch point, and a section $\mathcal{P}_2$ typical of reciprocal space. We compare in Fig. 4 the dynamic correlation function, normalized to unity at $t = 0$, at two temperatures with the predictions from Eq. (6) along the path $\mathcal{P}$. The excellent agreement of the curves across multiple temperatures, wave vectors, and times is good evidence that the stochastic model is sufficient to capture the relaxation behavior. It fails only at short times ($t \lesssim J^{-1}$, not shown in Fig. 4) on nodal lines, where it does not account for oscillatory spin wave contributions.

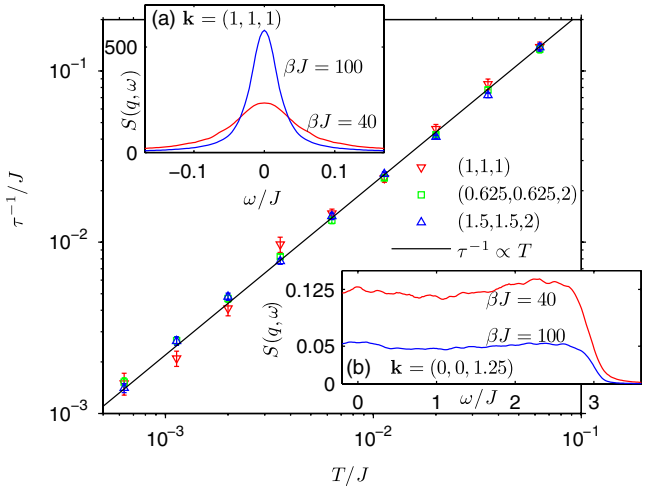

FIG. 2 (color online). Main panel: Decay rate of $S(\mathbf{q}, t)$ as a function of T at wave vectors as indicated. Upper inset: $S(\mathbf{q}, \omega)$ at $\beta J = 40$ (red curve) and 100 (blue curve), for $\mathbf{k} = (1, 1, 1)$. Lower inset: $S(\mathbf{q}, \omega)$ on a nodal line at $\mathbf{k} = (0, 0, 1.25)$.

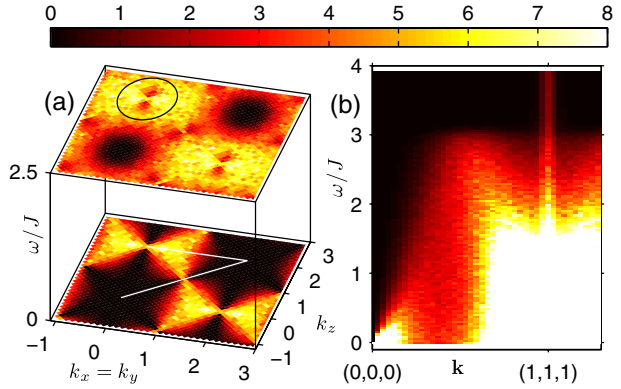

FIG. 3 (color online). Intensity map of $\beta S(\mathbf{q}, \omega)$ in the (q_x, q_x, q_z) plane at $\beta J = 500$. (a) Lower panel: Zero frequency (data divided by 1.25×10^5); white line is path $\mathcal{P}$. Upper panel: $\omega = 2.5J$; black circle is centered on a pinch point. (b) Section along path segment $\mathcal{P}_1$ (see text).

The stochastic model is microscopic and its main ingredients are a conservation law and the pyrochlore lattice structure. A long wavelength description is provided by the mapping to flux fields [7,8] and it is interesting to see how the dynamics translates under this mapping. Taking the low temperature, small q limit, the correlators for the continuum flux fields $\mathbf{B}(\mathbf{q}, t)$ implied by the stochastic model are

$$\langle B_i(\mathbf{q}, t) B_j(-\mathbf{q}, 0)\rangle \propto \left(\delta_{ij} - \frac{q_i q_j}{q^2}\right) e^{-8\Gamma\lambda T t} + \left(\frac{q_i q_j}{q^2} - \frac{q_i q_j}{q^2 + \xi^{-2}}\right) e^{-8\Gamma(Ja^2q^2 + \lambda T)t}.$$

This result can be derived from a Langevin equation for the continuum flux fields in which the "monopole density" $\rho = \nabla \cdot \mathbf{B}$ obeys a continuity equation $\partial_t \rho + \nabla \cdot \mathbf{j} = 0$, with monopole current density

$$\mathbf{j} = 8\Gamma\lambda T \mathbf{B} - 8\Gamma J a^2 \nabla\rho + \eta(t). \quad (8)$$

Here, the second term is the usual diffusion current arising from a density gradient, while the first describes response to an entropic force. This response involves a drift current of the magnetic charge density ρ in the field $\mathbf{B}$ that mimics electrical conduction in electrodynamics and is responsible for the flat relaxation rate. Related results have been obtained recently in a study of dynamics in spin ice, represented by the Ising antiferromagnet [15]. In this case monopoles are discrete and it has been argued that purely diffusive dynamics are insufficient to explain observations and a full description must include the network of Dirac strings between monopoles, which are essentially entropic, as well as dipolar interactions [15]. In spin ice, dipolar interactions lead to Coulomb-law forces between monopoles. By contrast, in Eq. (8) Coulombic forces appear purely entropically.

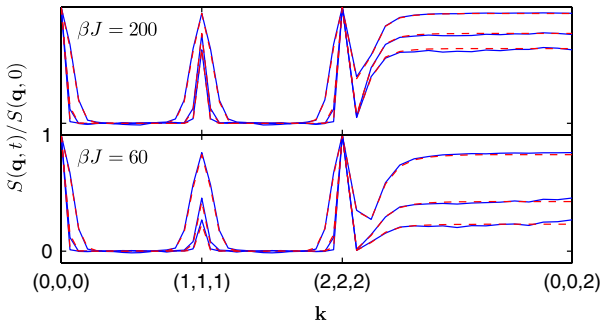

FIG. 4 (color online). Solid blue lines: Normalized correlation function $S(\mathbf{q}, t)/S(\mathbf{q}, 0)$. Dashed red lines: Prediction from Eq. (6) with $\Gamma = 0.167$, both shown at 3 times, t.

In summary, we have considered wave vector and frequency resolved dynamics of the classical pyrochlore antiferromagnet. The relaxational behavior is well captured by a stochastic model that conserves total spin. Spin diffuses with a diffusion constant independent of temperature, and entropic forces drive currents to relax configurations with a rate independent of wave vector and inversely proportional to temperature.

This work was supported in part by EPSRC Grant No. EP/D050952/1.

*conlon@thphys.ox.ac.uk

[1] P. W. Anderson, Phys. Rev. **102**, 1008 (1956).
[2] J. Villain, Z. Phys. B **33**, 31 (1979).
[3] A. P. Ramirez, Annu. Rev. Mater. Sci. **24**, 453 (1994).
[4] R. Moessner and A. P. Ramirez, Phys. Today **59**, No. 2, 24 (2006).
[5] R. Moessner and J. T. Chalker, Phys. Rev. B **58**, 12 049 (1998); Phys. Rev. Lett. **80**, 2929 (1998).
[6] B. Canals and D. A. Garanin, Can. J. Phys. **79**, 1323 (2001).
[7] S. V. Isakov, K. Gregor, R. Moessner, and S. L. Sondhi, Phys. Rev. Lett. **93**, 167204 (2004).
[8] C. L. Henley, Phys. Rev. B **71**, 014424 (2005).
[9] D. A. Huse, W. Krauth, R. Moessner, and S. L. Sondhi, Phys. Rev. Lett. **91**, 167004 (2003).
[10] M. J. Harris, M. P. Zinkin, and T. Zeiske, Phys. Rev. B **52**, R707 (1995).
[11] J. van Duijn, N. Hur, J. W. Taylor, Y. Qiu, Q. Z. Huang, S.-W. Cheong, C. Broholm, and T. G. Perring, Phys. Rev. B **77**, 020405(R) (2008).
[12] P. G. de Gennes, J. Phys. Chem. Solids **4**, 223 (1958).
[13] M. de Leener and P. Résibois, Phys. Rev. **152**, 318 (1966).
[14] A. Bunker, K. Chen, and D. P. Landau, Phys. Rev. B **54**, 9259 (1996).
[15] L. Jaubert and P. Holdsworth, Nature Phys. **5**, 258 (2009).
[16] J. Robert, B. Canals, V. Simonet, and R. Ballou, Phys. Rev. Lett. **101**, 117207 (2008).